AN ACCURATE ANALYTICAL MODEL FOR ELECTROMECHANICAL ENERGY CONVERSION IN A PIEZOELECTRIC CANTILEVER BEAM FOR ENERGY HARVESTING

Ahmadreza Tabesh and Luc G. Fréchette
Microengineering Laboratory for MEMS, Université de Sherbrooke,
2500 boul. Université, Sherbrooke, Québec, J1K 2R1, Canada

Abstract: This paper develops an accurate model for energy conversion in a piezoelectric cantilever beam. The conventional energy-based model assumes a linear voltage distribution along the piezoelectric beam thickness. It is shown that the voltage distribution must be approximated at least by a quadratic function. The validity of the model is experimentally verified and compared with the conventional model where applicable. The equivalent capacitance of a beam which is calculated based on linear and quadratic voltage distribution shows an approximately 40% relative discrepancy for PZT5A.This inaccuracy level is not negligible especially when the design of electrical energy harvesting is concerned.

Keywords Energy Harvesting, Piezoelectric Cantilever Beam, Piezoelectric Energy Conversion Model

I. Introduction

Piezoelectric energy harvesters are promising power supplies for wireless network nodes and remote low-power apparatuses. Energy conversion modeling of piezoelectric cantilever beam energy harvesters is conventionally developed based on the energy method by assuming a linear voltage distribution along the piezoelectric beam thickness (e.g. see [1], [2]). Such a model has been utilized as the basis for MEMS-scale design and efficiency analysis of energy harvesters [2], [3]. This paper shows that the linear voltage distribution assumption imposes inaccuracy by violating Maxwell's equations in the piezoelectric beam. This inaccuracy obviously impacts on design and efficiency analysis of piezoelectric beams in the context of energy harvesters. The presented approach includes a static model for a deflected piezoelectric cantilever beam and a model for dynamic operation of a vibrating beam. The static model is directly obtained from a simultaneous solution of Maxwell's equation, solid-mechanic equations, and constitutive equations of a piezoelectric cantilever beam. The dynamic model is developed by including a damping and inertial term to the mechanical equation. The effective mass is analytically calculated based on the Rayleigh-Ritz method [4]. The new model is validated by comparing it with experimental measurements on a piezoelectric cantilever beam.

II. Static Electromechanical Model of a Piezoelectric Cantilever Beam

A. Governing Equations

Figure 1 shows the schematic diagram of a 2-layer piezoelectric cantilever beam. The beam includes two thin piezoelectric ceramic sheets which are bonded to a center support vane. Thickness of the beam and the center vane are represented by T_b and t_c, respectively. The well-know assumptions of the Euler-Bernoulli theory of beams [5], [6] have been employed to develop an electromechanical model of the beam.

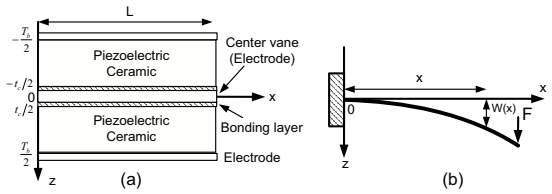

Fig. 1. *(a) Schematic diagram of a 2-layer piezoelectric beam (bimorph), (b) The bending piezoelectric element mounted in a cantilever beam configuration.*

The governing equations of a piezoelectric cantilever beam under a static condition are concluded from (i) Maxwell's electrostatic equations for the compound beam materials, (ii) force equilibrium of the cantilever beam, and (iii) the constitutive equations which associates electrical and mechanical properties of the beam materials. Applying the beam theory assumptions, the constitutive equations of a cantilever beam become [7]:

$$\begin{aligned} \epsilon_x &= s_{11}^E \sigma_x + d_{31} E_z \, \vec{a}_p \cdot \vec{a}_z \quad (a), \\ D_x &= \varepsilon_{11}^T E_x + d_{15} \tau_{xz} \, \vec{a}_p \cdot \vec{a}_z \quad (b), \\ D_z &= \varepsilon_{33}^T E_z + d_{31} \sigma_x \, \vec{a}_p \cdot \vec{a}_z \quad (c), \end{aligned} \tag{1}$$

where D and E represent electric displacement and electric field; ϵ, σ denote strain and stress. s^E, ε^T and d are the compliance coefficient at constant electric field , tension free electric permittivity, and coupling coefficient, respectively. Subscripts (1,2,3) are axes of the piezoelectric ceramic which are selected corresponding to (x, y, z). The constant unit vectors

The work of A. Tabesh was supported in part by the Canadian Natural Science and Engineering Research Council (NSERC) through a Postdoctoral Fellowship. E-mails: a.tabesh@utoronto.ca, lucf@alum.mit.edu .

$\vec{a}_z$ and $\vec{a}_p$ denote the positive direction of the z-axis and the poling direction of a piezoelectric ceramic, respectively. The piezoelectric beam can operate in series or parallel modes depending on the polling direction of the piezoelectric ceramics. In Fig. 1, the electric field and electric displacement components along the y-direction are zeros due to symmetry, *i.e.* $E_y = D_y = 0$. Thus, the potential function $v(x, z)$ is not a function of y. For the non-piezoelectric center vane, the coupling coefficients d_{ij} are zeros. Thus, Eqn. (1) reduces into decoupled equations that independently describe mechanical and electrical properties of the center vane. The free-charge density inside the piezo-electric cantilever beam, ρ_v, is zero. Therefore, electrostatic Maxwell's equations of the beam are:

$$\nabla \cdot D = \rho_v, \quad \rho_v = 0 \Rightarrow \quad \frac{\partial D_x}{\partial x} + \frac{\partial D_z}{\partial z} = 0, \tag{2}$$

$$\nabla \times E = 0 \Rightarrow \quad E_x = -\frac{\partial v(x,z)}{\partial x}, \quad E_z = -\frac{\partial v(x,z)}{\partial z}. \tag{3}$$

The simplified beam force equilibrium equation is:

$$\frac{\partial \sigma_x}{\partial x} + \frac{\partial \tau_{xz}}{\partial z} = 0. \tag{4}$$

From beam theory [5], [6], σ_x is a linear function of x and z, thus $\partial\sigma_x/\partial x$ in Eqn. (4) is only a function of z that means $\partial\tau_{xz}/\partial z$ has to be merely a function of z. Therefore, τ_{xz} must be a quadratic function of z. The cantilever beam in Fig.1(b) has a distribution of internal stresses which apply a total internal bending moment M at any position x. Static equilibrium constraint for the cantilever beam of Fig. 1 requires that $M = -F(L - x)$. M can also be determined by calculating the first moment of σ_x as given by

$$M = W\left(\int_{-\frac{T_b}{2}}^{-\frac{t_s}{2}} \sigma_{x_t} z dz + \int_{-\frac{t_s}{2}}^{\frac{t_s}{2}} \sigma_{x_m} z dz + \int_{\frac{t_s}{2}}^{\frac{T_b}{2}} \sigma_{x_b} z dz\right), \tag{5}$$

where σ_{x_t}, σ_{x_m}, and σ_{x_b} represent normal stress σ_x at the top, center, and bottom layers of the cantilever beam of Fig.1, respectively. Equations (1)-(5) completely describe the static electromechanical behavior of a piezoelectric cantilever beam. A possible solution for Eqn. (2) is to assume D_x is only a function of z and D_z is only a function x. Thus, from Eqn. (1b) and Eqn. (1c), E_x becomes only a function of z and E_z has to be a linear function of x and z. The above conclusions and Eqn. (3) indicate that

$$v(x, z) = \psi_0(x) + \psi_1(x)z + \psi_2(x)z^2, \tag{6}$$

where $\psi_0(x), \psi_1(x)$ and $\psi_2(x)$ are linear functions of x satisfying voltage boundary conditions and constitutive equations. Equations Eqn. (1) and Eqn. (5) can be solved for ρ and D_z utilizing $v(x, z)$ in Eqn. (6). Having ρ and D_z provide two coupled force and charge equations which model the energy conversion mechanism of a piezoelectric cantilever beam. The following sections elaborate these equations for series and parallel connection modes of a piezoelectric cantilever beam, individually.

B. Series Connected Piezoelectric Cantilever Beams

In a series connected piezoelectric beam the poling vector of the piezoelectric ceramic layers in Fig. 1 are oriented in opposite directions. Therefore, $\vec{a}_p \cdot \vec{a}_z = z/|z|$ where $|z|$ denotes the absolute value of z for $t_c/2 < |z| \leq T_b/2$. Assume that the voltage boundary conditions in Fig.1(a) are:

$$v(x, -T_b/2) = V/2, \; v(x, \pm t_c/2) = 0, \; v(x, T_c/2) = -V/2.$$

V is the potential difference between the top and bottom layers. It can be readily shown that:

$$v = \begin{cases} \frac{z}{|z|}\psi_0(x) - \psi_1(x)z - \frac{z}{|z|}\psi(x)z^2 & \frac{t_c}{2} \leq |z| \leq \frac{T_b}{2} \\ 0 & 0 \leq |z| \leq \frac{t_c}{2} \end{cases} \tag{7}$$

where

$$\psi_0(x) = \frac{V t_c}{2(T_b - t_c)} - \frac{T_b t_c \psi(x)}{4}, \;\; \psi_1(x) = \frac{V}{T_b - t_c} - \frac{(T_b + t_c)\psi(x)}{2}$$

satisfies the voltage boundary conditions for an arbitrary linear function $\psi(x) = \alpha_1 x + \alpha_0$ where α_1 and α_0 are two constants to be determined from the solution of the electromechanical equations. Substituting $\epsilon_x = -z/\rho$ and $E_z = -\partial v/\partial z$ in Eqn. (1a) and solving for σ_x, we obtain

$$\sigma_x = \begin{cases} -\frac{z}{s_{11}^E \rho} + \frac{z}{|z|}\frac{d_{31}}{s_{11}^E}\frac{\partial v}{\partial z} & \frac{t_c}{2} < |z| \leq \frac{T_b}{2} \\ -\frac{z}{s_{11}^D \rho} & 0 \leq |z| \leq \frac{t_c}{2} \end{cases}. \tag{8}$$

Assuming $(t_c/T_b)^n$ for $n \geq 2$ is negligible in comparison to 1, substituting for σ_x from Eqn. (8) in Eqn. (5) and solving Eqn. (5) for ρ, we obtain

$$\frac{1}{\rho} = \frac{-12 s_{11}^E M}{W T_b^3} + 3 d_{31}\frac{V}{T_b^2}\frac{t_c}{T_b} + \frac{1}{2} d_{31}\psi(x)(1 - 3\frac{t_c}{T_b}). \tag{9}$$

Replacing for ρ from Eqn. (9) in Eqn. (8) and substituting its result in Eqn. (1c) provides D_z in terms of $\psi(x)$. It can be shown that $\psi(x)$ vanishes z in D_z by selecting

$$\alpha_1 = \frac{6 d_{31} F}{\varepsilon_{33}^T W T_b^3 \left(1 - \frac{3}{4}k_{31}^2(1 + \frac{t_c}{T_b})\right)}, \;\; \alpha_0 = \frac{6 d_{31} L F + \frac{3}{2} d_{31}^2 W T_b V (1 + \frac{t_c}{T_b})}{\varepsilon_{33}^T W T_b^3 \left(1 - \frac{3}{4}k_{31}^2(1 + \frac{t_c}{T_b})\right)}.$$

$k_{31} = \sqrt{d_{31}^2/\varepsilon_{33}^T s_{11}^E}$ denotes the piezoelectric coupling factor. Employing the above α_1 and α_0, and neglecting $(t_c/T_b)^2$ comparing to 1, the D_z inside the beam simplifies to

$$D_z = \begin{cases} \frac{1}{\alpha_p}\left(\frac{3 d_{31}(1 + \frac{t_c}{T_b})(L - x)F}{W T_b^2} + \frac{\varepsilon_{33}^T V}{T_b - t_c}\right) & \frac{t_c}{2} < |z| \leq \frac{T_b}{2} \\ 0 & 0 \leq |z| \leq \frac{t_c}{2} \end{cases} \tag{10}$$

where $\alpha_p = 1 + 0.25k_{31}^2/(1 - k_{31}^2)$. Applying Gauss's law to the upper electrode, the electrode total free-charge Q is:

$$Q = \int_0^L \int_{-\frac{W}{2}}^{\frac{W}{2}} D_z dy dx = \frac{1}{\alpha_p}\left(\frac{3 d_{31} L^2}{2 T_b^2} F + C_{s_0} V\right). \tag{11}$$

$C_{s_0} \triangleq \varepsilon_{33}^T LW/(T_b - t_c)$ is the tension free capacitance of the series connected piezoelectric beam. The charge can be expressed in terms of V and the beam tip deflection, $u \triangleq w(L)$,

by solving the differential equation $d^2w/dx^2 = 1/\rho$ for $w(x)$. Applying the boundary conditions $w(0) = dw/dx|_{x=0} = 0$ to this differential equation, we obtain

$$u = \int_0^L \int_0^x \frac{1}{\rho(\tilde{x})} d\tilde{x} dx = \frac{1}{\alpha_p} \left(\frac{4 s_{11}^E L^3}{W T_b^3} F + \frac{3 d_{31} L^2}{2 T_b^2} V \right) \quad (12)$$

Solving Eqn. (12) and Eqn. (11) for F and Q, the static model of the series piezoelectric cantilever beam is obtained as follows:

$$F = K_s u - \Theta_s V \quad (13)$$
$$Q = \Theta_s u + C_s V \quad (14)$$

where

$$K_s = \frac{\alpha_p W T_b^3}{4 s_{11}^E L^3}, \quad \Theta_s = \frac{3 d_{31} W T_b}{8 s_{11}^E L} (1 + \frac{t_c}{T_b}), \quad C_s = \frac{1}{\alpha_p} C_{s0} \left(1 - \frac{9}{16} k_{31}^2 (1 + \frac{t_c}{T_b}) \right). \quad (15)$$

In expression for C_s, the term including $(t_c/T_b)^2$ is neglected in comparison to 1. The coefficients K_s, Θ_s, and C_s are defined as the stiffness, the coupling, and the equivalent capacitance associate to a series piezoelectric cantilever beam.

C. Parallel Connected Piezoelectric Cantilever Beams

The piezoelectric ceramic layers have similar poling directions in the parallel mode such that $\vec{a}_p \cdot \vec{a}_z = 1$ in Eqn. (1) in the both top and bottom layers. In parallel mode, the voltage boundary conditions of Fig. 1(a) are

$$v(x, \pm T_b/2) = V, \quad v(x, \pm t_c/2) = 0,$$

where V is potential difference across top or bottom layer and center electrode. The quadratic function

$$v = \begin{cases} \psi_0(x) + \frac{z}{|z|} \psi_1(x) z + \psi(x) z^2 & \frac{t_c}{2} \le |z| \le \frac{T_b}{2} \\ 0 & 0 \le |z| \le \frac{t_c}{2} \end{cases} \quad (16)$$

where

$$\psi_0(x) = -\frac{V t_c}{(T_b - t_c)} + \frac{T_b t_c \psi(x)}{4}, \quad \psi_1(x) = \frac{2V}{T_b - t_c} - \frac{(T_b + t_c)\psi(x)}{2}$$

satisfies all of the voltage boundary conditions in parallel mode, with $\psi(x) = \alpha_1 x + \alpha_0$. Analogous to the series mode analysis α_1, α_0 are constants to be determined from the solution of the electromechanical equations. Following a similar procedure to that of elaborated for series mode, it can be shown that in parallel mode:

$$F = K_p u - \Theta_p V \quad (17)$$
$$Q = \Theta_p u + C_p V \quad (18)$$

where

$$K_p = \frac{\alpha_p W T_b^3}{4 s_{11}^E L^3}, \quad \Theta_p = \frac{3 d_{31} W T_b}{4 s_{11}^E L} (1 + \frac{t_c}{T_b}), \quad C_p = \frac{1}{\alpha_p} C_{p0} \left(1 - \frac{9}{16} k_{31}^2 (1 + \frac{t_c}{T_b}) \right). \quad (19)$$

and $C_{p_0} \triangleq 4 \varepsilon_{33}^T LW/(T_b - t_c)$. Comparing model coefficients between the series and parallel modes indicates that $K_p = K_s$, $\Theta_p = 2\Theta_s$, and $C_p = 4C_s$.

D. Linear Voltage Assumption

An approximate model can be developed based on a linear voltage distribution (constant electric field) inside the piezoelectric material [1], [2]. It is informative to compare this approximate model with the model developed in the previous section. The models are only compared in parallel mode. Assuming V is the potential difference between the top/bottom and the center electrodes in Fig. 1(a), then the linear potential distribution is $v = \psi(z)V$ where

$$\psi(z) = \begin{cases} \frac{z}{|z|} \cdot \frac{(2z + t_c)}{T_b - t_c} & \frac{t_s}{2} \le |z| < \frac{T_b}{2} \\ 0 & \frac{t_s}{2} \le |z| \le \frac{T_b}{2} \end{cases} \quad (20)$$

Utilizing the energy method for a piezoelectric cantilever beam with linear voltage distribution [1], [2], the capacitance is:

$$C = \int_{V_p} \varepsilon_{33}^S \psi^2(z) dV_p = 4 \frac{\varepsilon_{33}^S W L}{T_b - t_c}. \quad (21)$$

where V_p represents piezoelectric volume and ε_{33}^S is the dielectric permittivity when the strain is zero. Comparing C in Eqn. (21) with the equivalent capacitance C_p in Eqn. (19) shows discrepancy due to linear voltage assumption. Using the parameters of commercially available piezoelectric material [7], it can be shown that the level of discrepancy can be more that 40% (e. g. 45.8% for PZT5A).

E. Quasi-Static Model of a Vibrating Piezoelectric Beam

Dynamic behavior of a vibrating beam can be modelled by adding a damping and an inertia term to the static model. Such a quasi-static model can accurately model the beam small-signal vibrations at frequencies well below of resonant frequencies of the piezoelectric material [6], [7]. The quasi-static model is:

$$M_{eff} \ddot{u}(t) + C_d \dot{u}(t) + K u - \Theta V(t) = F, \quad (22)$$
$$\Theta u(t) + C V(t) = Q(t), \quad (23)$$
$$I(t) = \frac{dQ(t)}{dt}, \quad (24)$$

where M_{eff}, C_d are effective mass and damping of the beam, F represents an applied external force, and $I(t)$ is electric current into the piezoelectric beam. Using Rayleigh-Ritz method [5] the effective mass is $M_{eff} = 33 M_b/144$ where M_b is physical mass of the beam. C_d can be experimentally determined from the beam frequency response or estimated analytically in terms of drag, squeezing, flexural, and structural damping components [2]. Here, we measure resonant frequency, ω_n, and C_d of the beam using a procedure based on phasor analysis at a steady-state condition. A phasor $\bar{x} = |x| \angle x$ represents amplitude (peak value) and phase of $x(t)$ in a complex plane. The phasor representation of Eqn. (22) for the beam is:

$$(K - \omega^2 M_{eff} + j\omega C_d)\bar{u} - \Theta \bar{V} = \bar{F}. \quad (25)$$

Assume that the beam at the tip is freely vibrating therefore $\bar{F} = 0$ in Eqn. (25). At the resonant frequency ω_n, $K = \omega_n^2 M_{eff}$ and Eqn. (25) becomes:

$$j\omega_n C_d \bar{u} = \Theta \bar{V}. \quad (26)$$

Equation Eqn. (26) illustrates that i) the resonant frequency is the frequency at which $\bar{V}$ and $\bar{u}$ have 90° phase shift, and ii) C_d is obtained by solving Eqn. (26) for C_d as given by:

$$C_d = -\left(\frac{\Theta|\bar{V}|}{\omega_n|\bar{u}|}\right). \tag{27}$$

The negative sign in Eqn. (27) is inserted since $\Theta \leq 0$.

III. Model Verification

A. Experimental Setup

Figure 3 shows the schematic diagram of an experimental setup for verifying the model. The setup includes a series piezoelectric cantilever beam connected to a function generator through a power amplifier. The applied voltage across the beam electrodes is directly measured and monitored. The current through the beam and displacement at the tip of the beam are measured via current and optical laser micrometer sensors. The voltage, current, and displacement are simultaneously monitored and measured on a digital oscilloscope. The measured quantities are used to calculate resonant frequency and damping coefficient of the model.

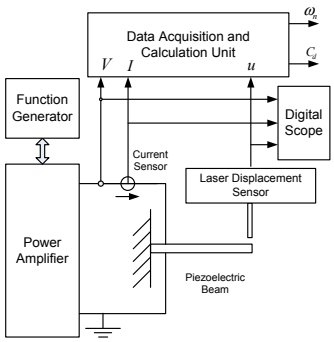

Fig. 2. *Schematic diagram of the experimental setup*

B. Experimental Verification of the Model

To verify the model, the displacement transfer function and current transfer function are defined based on Eqn. (22) to Eqn. (24) assuming $F = 0$. The displacement transfer function, $H_d(s)$, is defined the ratio of displacement to the voltage and theoretically obtained by applying the Laplace transformation to Eqn. (22) as:

$$H_d(s) \triangleq \frac{u}{V} = \frac{\Theta}{M_{eff}s^2 + C_d s + K}. \tag{28}$$

The current transfer function, $H_i(s)$, is defined as the ratio of I to V and is obtained by substituting for u from Eqn. (28) in Eqn. (23) in the Laplace domain:

$$H_i(s) \triangleq \frac{I}{V} = Cs + s\Theta H_d(s) \tag{29}$$

To obtain $H_d(j\omega)$ and $H_i(j\omega)$ theoretically, K, Θ, and C are calculated from Eqn. (15). The resonant frequency is calculated from $\omega_n = \sqrt{K/M_{eff}}$. ω_n and C_d are also experimentally measured using the procedure elaborated in Section II.E. To verify the model, $H_d(j\omega)$ and $H_i(j\omega)$ are also obtained

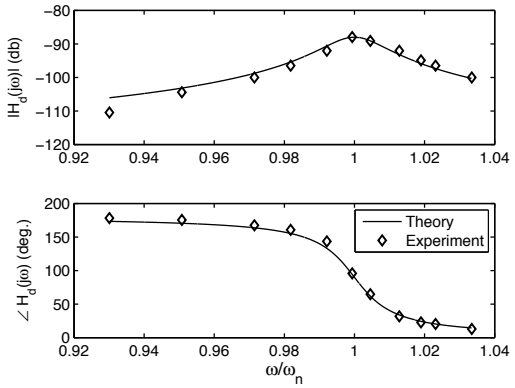

Fig. 3. *Frequency response of $H_d(j\omega)$*

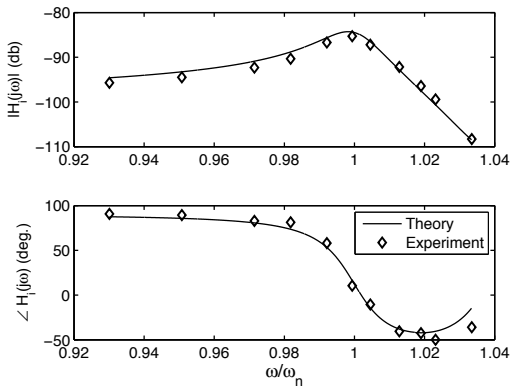

Fig. 4. *Frequency response of $H_i(j\omega)$*

from measured data as follows. The frequency of the input voltage is varied about the resonant frequency at a fixed amplitude. Then, the amplitude and phase shift of u and I with respect to V are measured to obtain $H_d(j\omega)$ and $H_i(j\omega)$ as defined in Eqn. (28) and Eqn. (29). Figures 3 and 4 show the frequency response of $H_d(j\omega)$ and $H_i(j\omega)$ with respect to normalized frequency of ω/ω_n. Each figure compares the frequency response of the model developed herein with that of experimentally obtained based on measured data. Consistency between theoretical and experimental data in Fig. 3 verifies the validity of using the quasi-static model in Eqn. (22) for the vibrating piezoelectric beam. It also shows the accuracy of the proposed procedure based on Eqn. (26) and Eqn. (27) for measuring the resonant frequency ω_n and damping coefficient C_d. Consistency among $H_i(j\omega)$ and measured data in Fig. 4 verifies the accuracy of the model using the quadratic voltage distribution.

References

[1] H. A. Sodano, G. Park, and D. J. Inman, "Estimation of Electric Charge Output for Piezoelectric Energy Harvesting," *Strain* (2004) 40, 49-58.

[2] N. E. duToit, B. L. Wardle, and S. G. Kim, "Design Considerations for MEMS-Scale Piezoelectric Mechanical Vibration Energy Harvesters," *Integrated Ferroelectrics*, 71: 121 − 160, 2005.

[3] Y. C. Shu, and I. C. Lien, "Efficiency of energy conversion for a piezoelectric power harvesting system," *J. Micromech. Microeng.* (2006) 16, 2429 − 2438.

[4] W. T. Thomson , "*Theory of Vibration with Applications* ,"Nelson Thornes Ltd., 1988.

[5] S. P. Timoshenko, J. N. Goodier,"*Theory of Elasticity,*"McGraw Hill,1970.

[6] S. D. Senturia,"*Microsystem Design,*" Kluwer Academic Publishers, 2001.

[7] J. Yang,"*An Introduction to the Theory of Piezoelectricity* ,"Springer, 2005.